Social interactions drive efficient foraging and income equality in groups of fish

Roy Harpaz[1] and Elad Schneidman[1†]

[1]Department of Neurobiology, Weizmann Institute of Science, Rehovot, Israel

Summary

Social foraging is considered to be a prominent advantage of living in a group. The ability to track the joint behavior of groups of animals has allowed for detailed characterization of individual traits and functional interactions between group members. Several theoretical models have explored collective foraging strategies, their relation to group composition, and the distribution of available resources. However, a quantitative link between models of the interactions among individuals that drive collective behavior, and social foraging by real groups of animals is still missing. Here, we tracked groups of adult zebrafish while foraging freely in open arena, and inferred from the data the functional interactions that govern their behavior. We found that fish showed stereotypical maneuvers when consuming food, which attracted neighboring fish to that location. We then devised mathematical models of interacting foragers based on attraction to consumption events, which accurately described foraging of real fish at the level of the individual and as a group. We show that such social interactions allow fish to combine individual and social information in an efficient manner, increasing foraging efficiency of groups and individuals - almost to the predicted optimum. We further show that such social attraction-based strategy would be beneficial for individual fish even if other group members were not using a similar strategy, and that the inferred social interaction rules promote income equality among the members of the group. Our results demonstrate how local interaction rules employed by individuals may underlie highly efficient and robust foraging strategies for the group, and emphasize the role of data driven models in linking mechanistic interactions and theoretical predictions.

[†] For correspondence: elad.schneidman@weizmann.ac.il

Introduction

Living in a group has clear potential benefits, including expansion of sensory sensitivity [1–6], sharing of responsibilities and resources [7–9], collective computation [3–6, 10–12], and the potential for symbiotic relations between members that would allow for specialization by individual members [9, 13]. Understanding the interactions among individuals that give rise to macroscopic behavior of groups is therefore central to the study and analysis of collective behavior in animal groups and other biological systems.

Group foraging is a prominent example of collective behavior, and social interactions among members have been suggested to increase foraging efficiency of groups by allowing individuals to combine private and social information about the location of resources and their quality [1, 14–19] (see however [20, 21] for adverse effects of social information). It is commonly assumed that individuals can infer the location and quality of resources from their neighbors' behavior [17, 22–24]. It is unclear however, what foraging strategy should individuals employ in a social context in order to increase foraging efficiency and what kind of interindividual interactions may support it [16].

Theoretical models were used to study foraging dynamics using different strategies, including producer-scrounger dynamics [25] and information sharing [26–28]. These models explored the efficiency of the underlying strategies, their evolutionary stability, and the effects of group composition and resource distributions [25, 27, 29–31]. Experimental work, in the field and in the lab, aimed to identify the interaction rules that govern social foraging [11, 24, 32–35] and their dependence on factors such as the distribution of resources, phenotypic diversity among foragers, animal personality, and mixed species foraging strategies [36–39]. However, the connections between the theoretical models and interaction rules of individuals in real groups are missing, as the predictions of theoretical models were not tested against experimental data of specific groups or individuals [25, 40–43].

The ability to track the behavior of groups of individuals with high temporal and spatial resolution under naturalistic conditions [44–48] allows for quantitative study of foraging models and individual behavior. Here, we studied food foraging by groups of adult zebrafish in an open arena. We inferred social interaction rules between fish and compared several mathematical models of group foraging, based on these rules and the swimming statistics of individual animals. We explored the performance of these models in terms of foraging dynamics and efficiency of food consumption of the group and of individuals. Our data driven approach allowed us to link local interactions between conspecifics to social foraging strategies, to show that real groups of fish

forage in a nearly optimal manner, and to analyze income inequality among group members.

Results

We studied free foraging of single adult zebrafish and of groups of 3 or 6 fish, in a large circular arena with shallow water, where small food flakes were scattered on the surface (Fig. 1, S1A, and Methods). The trajectories and heading of individual fish, the position of flakes, and food consumption events were extracted from video recordings of these experiments using a tracking software that was written in house [49]. Tracking of fish identities in the videos were verified and corrected using the *IdTracker* software [44]. Fish were highly engaged in the foraging task and consumed all flakes in less than 2 minutes in most cases (Fig. 1B, movie 1). The number of recorded consumption events varied between groups, since in many cases fish ate only a part of a flake or flakes disintegrated into smaller parts (Fig. S1B).

The time it took a group of k fish to consume n flakes, which we denote by $T_k(n)$, was accurately predicted using a simple exponential model, such that

$$ln\hat{T}_k(n) = \frac{n}{b_k} + a_k \qquad (1)$$

where parameters b_k (the "consumption rate" of the fish) and a_k (time to detection of the first flake) were found numerically to minimize the mean squared error between the model predictions and the data. The correlation between the observed $T_k(n)$ and model predictions $\hat{T}_k(n)$ was very high, with median r^2 values: 0.94 [0.09], 0.96 [0.04], 0.96 [0.05] - for groups of 1, 3, and 6 fish respectively (brackets show interquartile range). Larger groups consumed the flakes faster than would be predicted just from having a larger number of foragers (Fig. 1B-C), which we tested using a model of independent foragers (Fig. S1C, see models below). Thus, the foraging fish were aware of the behavior of the other fish and were affected by them.

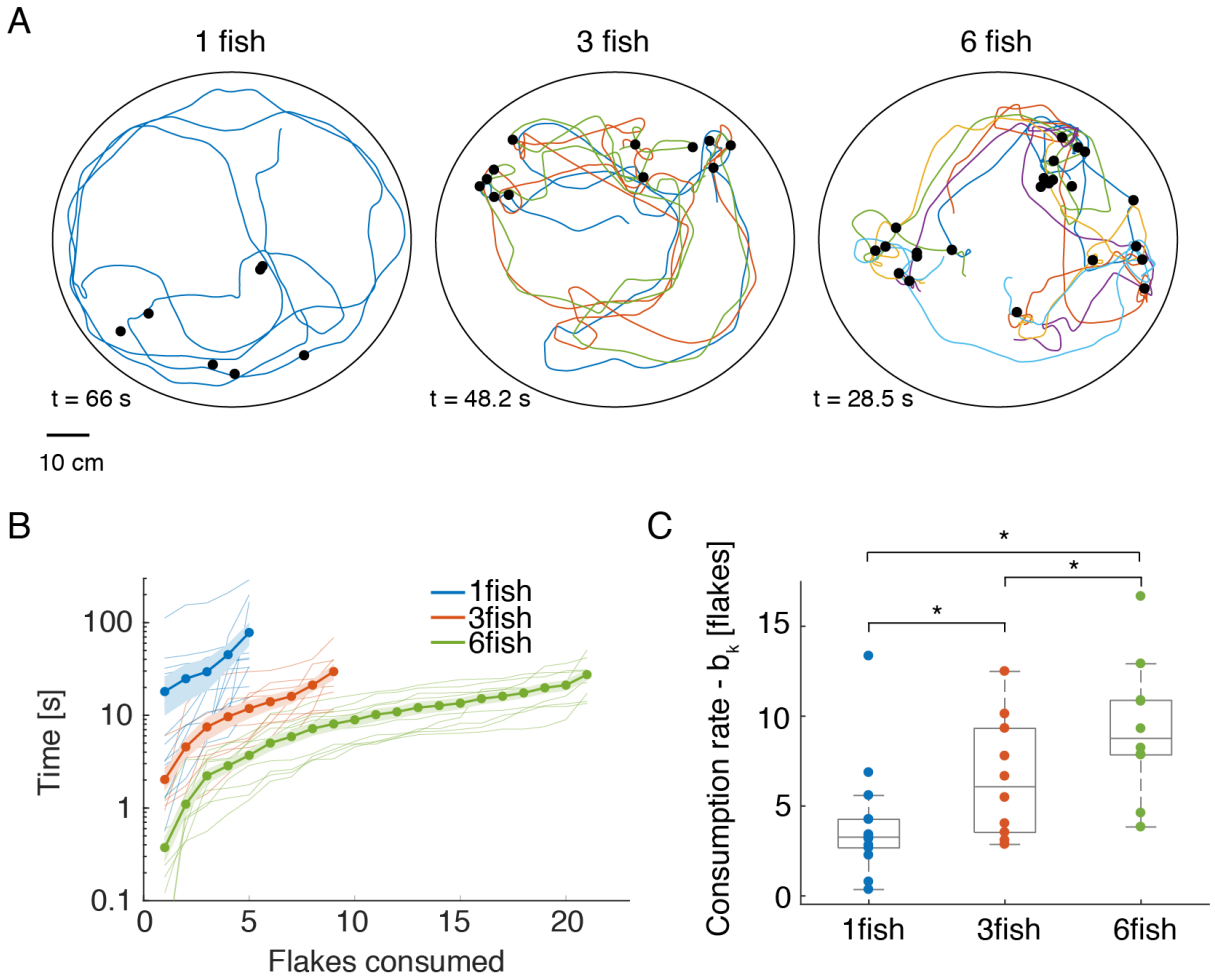

Figure 1: Individual and group foraging in adult zebrafish. A. Example trajectories of groups of 1, 3, and 6 fish foraging for food flakes. Colored lines show the trajectories of individual fish, black dots show the location of flakes consumed by the fish. **B.** Time of consumption of the ith flake in the arena is shown for each of the groups tested (thin lines, show N=14,10, and 10 groups of 1,3, and 6 fish) overlaid with the mean of all groups for every group size (thick line); light shadings represent SEM. **C.** Boxplots show the rate of flake consumption b (see main text) that were fitted for each of the groups shown in A. Middle horizontal lines represent median values and box edges are the 1st and 3rd quartiles (* denotes P<0.05 Wilcoxon rank-sum test, N = 14,10,10 fish).

To explore the nature of the dependency between foraging fish, we analyzed individual swimming behavior before and after flake consumption events. Fish performed salient and stereotypic maneuvers around the consumption of food items: They increased their speed when approaching food and then abruptly turned in the process of consuming it (Fig. 2A-C and Movie 2). This maneuver was characterized by a decrease in speed and an increase in the curvature of the trajectory (Fig. 2B,C, S2A). We found that for most groups of 3 and 6 fish analyzed (75%), neighboring fish responded to these salient behaviors and were more likely to visit areas of recent flake consumption within 1s (Fig. 2D, E), much more than expected by chance (P<0.001

and P<0.05 for 3 and 6 fish, t-test). Fish were less attracted to the location of a neighbor's consumption maneuver if flakes were more abundant in the arena (Fig. S2B). To confirm that these salient behavioral changes attracted fish to previous consumption areas, and not a physical trace of the flake, we also analyzed ``pseudo consumption events", where fish performed speed changes similar to those seen near flake consumption, but with no food present (see Methods). Neighboring fish were indeed attracted to such pseudo-consumptions events, affirming that fish responded to the specific behavior of their neighbors (Fig. S2C, D).

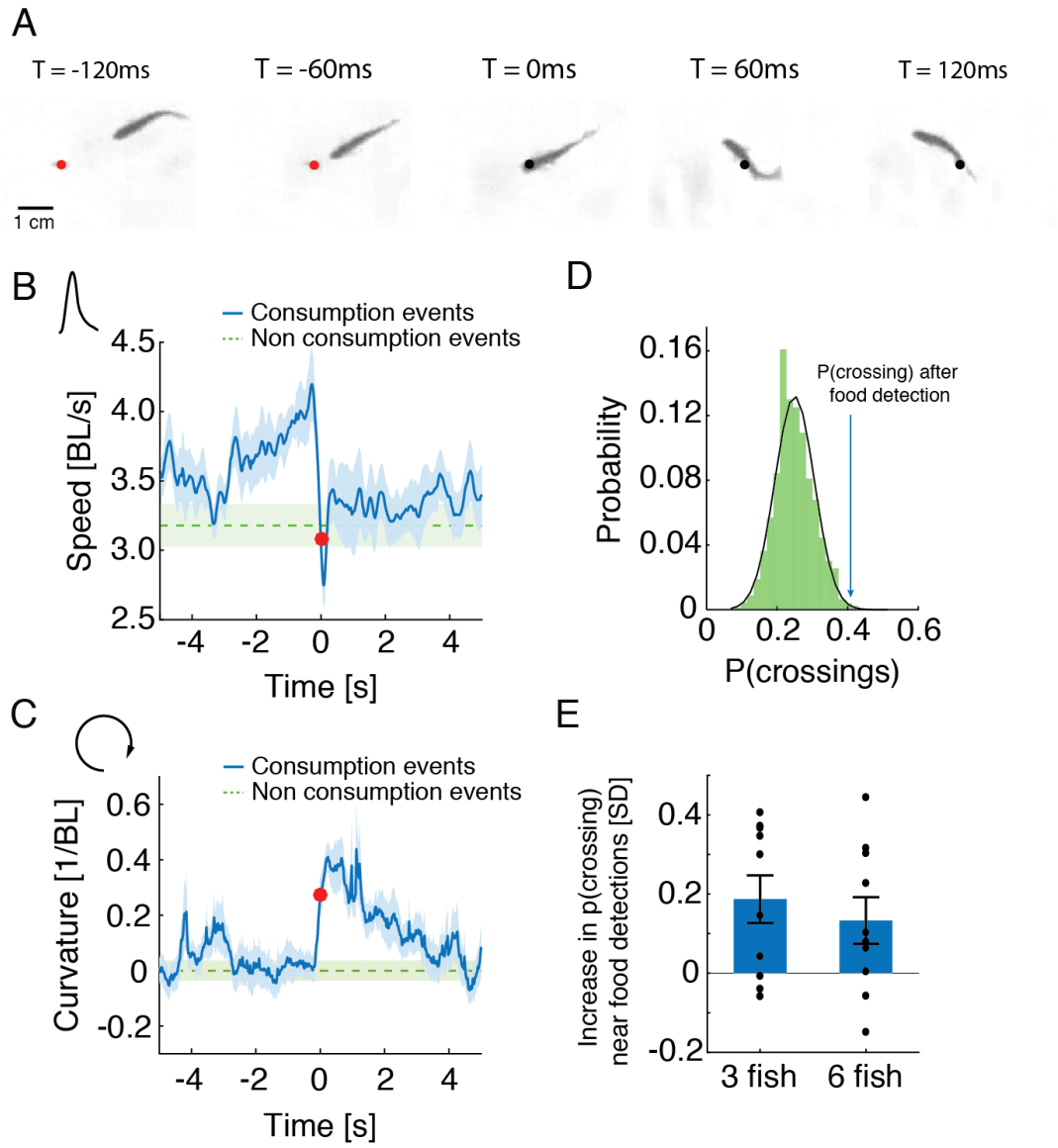

Figure 2: Stereotypical maneuvers before and during flake consumption by one fish attracts its neighbors. **A.** An example of the stereotypical behavior of one fish (in a group of 3) showing flake detection and consumption. Flake position is shown by a red circle before consumption and by a black circle after it has been eaten. **B-C.** Stereotypical behaviors around flake consumption (which we set as time 0 and mark by a red dot) include a transient increase in speed (shown in body length (BL) per second), followed by a sharp

decrease (B); this is accompanied by an increase in the curvature of the trajectory (C). Bold blue lines are mean speed and curvature profiles over all detection events of all groups of 3 fish, and dotted green line show a reference value calculated from random points along the trajectories not related to consumption events (curvature values were normalized such that the average curvature is zero). Light blue and green shadings show SEM. **D.** Probability of neighbors to cross within 2 BLs from the location of a previous flake consumption, in the 1s following consumption, for one group of 3 fish (blue arrow), compared to the distribution of such neighbor crossing events, ignoring flake consumptions (Methods). This reference distribution of crossings is well fitted by a Gaussian distribution (mean = 0.25, SD = 0.056), which is shown by a black overlaid line. **E.** Crossing probabilities for groups of 3 and 6 fish show significant increase from the baseline neighbor crossing distribution of each group, similar to C; 0 represent the mean of the baseline crossing distributions, error bars represent SEM.

To study the implications of attraction to locations of feeding by other fish, we simulated foraging groups of fish with social interactions and without it (see Methods). Simulations were based on the swimming characteristics of real fish and the empirical spatial distributions of flakes (Fig. 3A,B). We compared two models, shown in Fig. 3C-D and Box 1: (a) An independent foraging model where fish searched for food in the arena with no social interactions (which we denote by *IND*), and (b) A foraging model in which fish were attracted to locations where neighbors recently consumed food (*ATT*). In both models, the swimming trajectories of each simulated fish were constructed by successive drawing from the distribution of step sizes (the length of the path traveled on discrete `bouts' according to our segmentation of real fish trajectories; Fig. 3A,B) and turning angles (change of heading angle between two discrete bouts) of a specific real fish in the group (Fig. 3A,B). This amounts to a random walk model with an average step size 2.85 ± 1.7 body lengths (BL) and nearly symmetric turning values with an average of $1.8° \pm 49.7°$ in groups of 3 fish, and an average step size of 3.1 ± 1.9 BL, and average turning angle $-0.5° \pm 46°$ for group of 6 fish (Fig. S3A-B). However, if a flake was within the sensory range of detection by a fish, which we denote by D_f, that fish oriented itself directly towards the flake with a probability that decreased with the distance to the flake (see Box 1). In the *ATT* model, the direction of motion of each fish was also influenced by flake consumption of neighbors: If a flake was consumed by a neighbor within the sensory range of neighbor detection, D_n, within the last 5 movement steps (typically lasting 2-3 seconds, which was the estimated approach time of real fish to a flake based on changes in speed near flake consumptions, see Fig. 2B and Methods) - the observing fish oriented towards that location with a probability that decreased with distance to the detection point (see Fig. 3C, D for illustration).

Box 1

(1) Independent model (IND):

if a flake is closer than D_f

orient towards flake with $p = e^{-d_f/D_f}$. d_f distance to flake, D_f maximal range of detection

else

draw new turning angle and step length from the empirical distributions of that fish

(2) Neighbor attraction model (ATT):

if a flake is closer than D_f

act as in IND model

else if a flake was consumed by a neighbor in a location that is closer than D_n in the last τ time steps,

Orient towards detection point with $p = e^{-d_n/D_n}$ where d_n is distance to neighbor, and D_n maximal range of detecting neighbors

else

draw new turning angle and step length from the empirical distributions of that fish

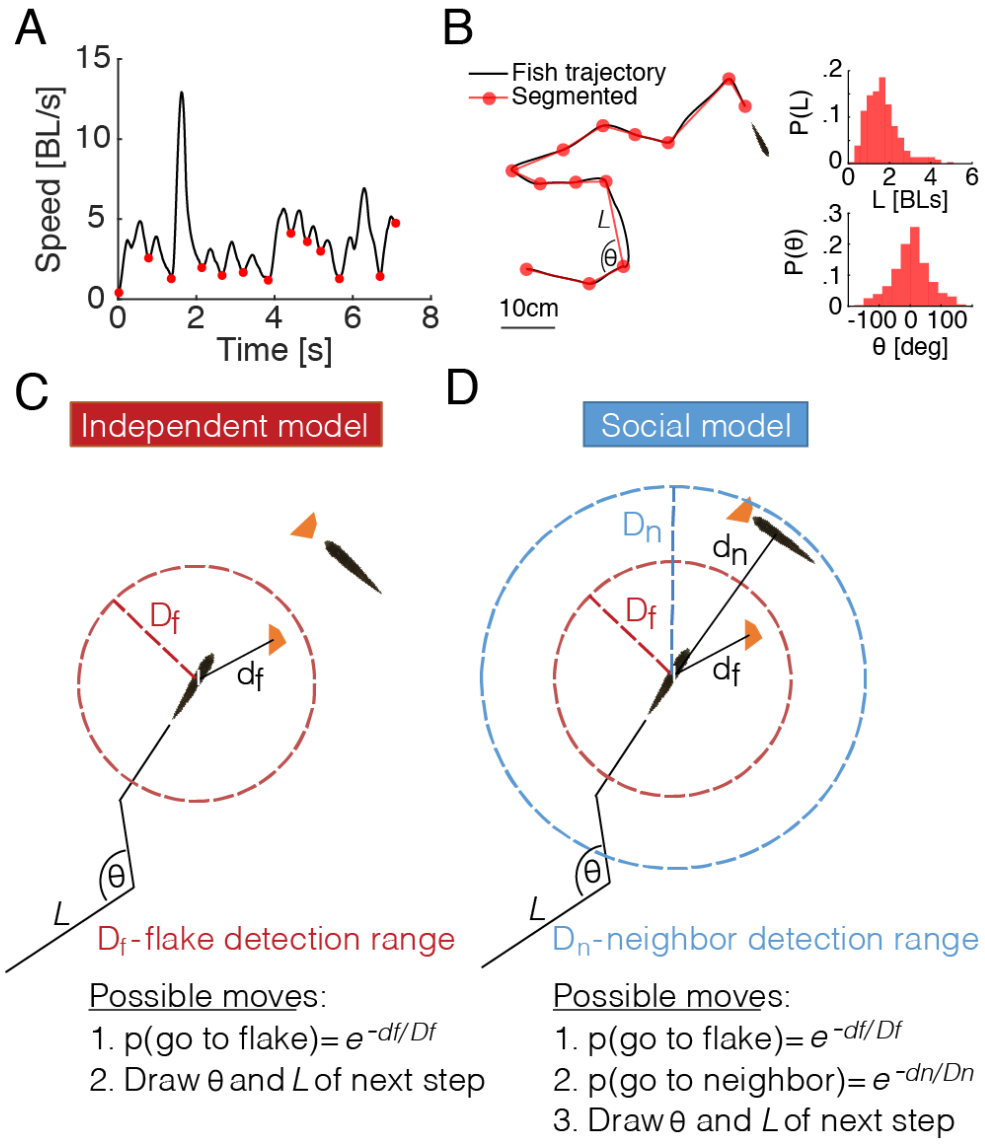

Figure 3: **Comparing social and independent foraging using model simulations. A.** An example of the speed profile of an individual fish in a group. Red dots mark local minima and are used to segment the continuous motion into discrete events. **B.** Left: A snippet of a fish trajectory, corresponding to the speed profile in A and its segmentation into discrete steps (red line). Right: Distributions of step size L and angle change θ, between discrete steps over 3 fish in one of the groups (Methods). **C.** A drawing showing the independent model of fish foraging (*IND*): At each time step, if a flake is present within a fish's detection range ($d_f < D_f$ – red circle), it will cause the fish to orient towards that flake with a probability p(go to flake). Otherwise, the fish will choose a new step size *L* and an angle change θ from the distributions that were estimated using real fish swimming (as in B). **D.** A drawing of the social model of fish foraging: In addition to flake detection as in C, each fish can also detect consumption of flakes by other fish if it is within the neighbor detection range ($d_n < D_n$ blue circle). If such an event occurred, the observing fish will attract to that point with probability p(go to neighbor).

For each real group of fish, we simulated their behavior 100 times, starting from their empirical initial positions and using the actual flake distributions, for a range of possible values of the model parameters D_f and D_n (Fig. 4A). For each set of parameter values D_f, D_n, we use the distribution of consumption times of flake k over the simulations, to assess the probability of observing a sequence of consumption events on real data traces. Thus, the probability of the ith consumption event to occur at time T is given by its value from the simulations of the model, $P_{D_f,D_n}(T_{data}(i))$, and the probability of a sequence of consumption times is given by the product of the probabilities of the individual events $\prod_i P_{D_f,D_n}(T_{data}(i))$. The log likelihood of the model is then given by

$$log\ P_{D_f,D_n}(T_{data}(1), T_{data}(2), \dots) = \sum_i log\ P_{D_f,D_n}\big(T_{data}(i)\big) \qquad (2)$$

where $T_{data}(i)$ is the actual consumption time of the ith flake, and the probability *P* is the distribution of consumption times of the ith flake over all simulations for a specific set of model parameters D_f, D_n. We found that the likelihood of the attraction-based models was much higher than that of the independent models (Fig 4C-F): The median of the likelihood ratios was 11 [4,17] for groups of 3 fish and 445 [2, 6577] for groups of 6 fish (brackets show 1st and 3rd quartiles). When comparing the mean squared error (MSE) between real and predicted flake consumption times, the ATT model showed a significant reduction in error compared to the IND model (10 ± 15% and 30 ± 31% for groups of 3 and 6 fish; Fig S4A). The flake detection parameter values, D_f, that gave the best fit to real groups were relatively small for both models (~3 BL), and detection ranges of neighbor feeding in the *ATT* model, D_n, were about 4 times larger (~12 BL)(Fig. S4B). In addition, D_n values of the best fitted models had a significant positive correlation with the estimated probability of fish in the corresponding real group to swim to the locations where their neighbors fed (Fig. S4C, Fig. 2E). Notably, groups simulated with the *ATT* model had markedly different swimming patterns than the *IND* groups: The interacting fish exhibiting more coherent group movement, and ~33% more straight swimming segments (Fig. 4A-B). The attraction-based model reproduced additional features of foraging groups, such as long delays in detection times when flakes clustered in a few locations (Fig. 4A), that were not captured by the independent model (Fig. 4E). Thus, the *ATT* model gave an accurate approximation to group behavior.

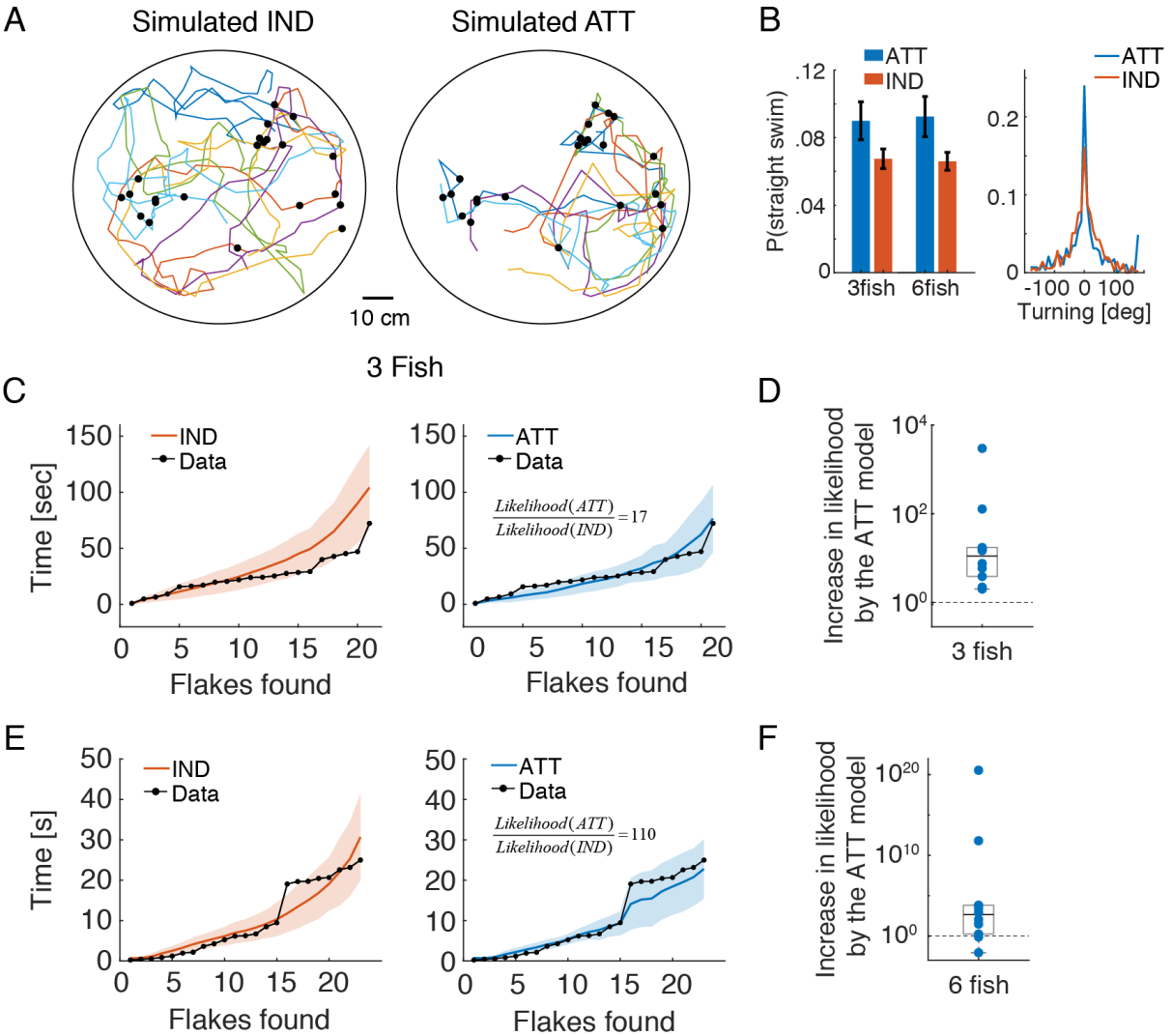

Figure 4: Attraction based models show the best fit to real foraging groups. A. Example trajectories from foraging simulations of a group of 6 fish, for the *IND* (left) and *ATT* (right) models that gave the best fit to real group foraging (i.e. maximized the log-likelihood of the models given the data, see eq. 2). Colored lines show different fish and black dots are flake positions. **B.** Probability to swim straight in simulated groups, estimated from the turning angle distributions (right), was significantly higher for the *ATT* model (P<0.01 and P<0.05 for groups of 3 and 6 fish respectively, t-test for matched samples, N=10,10). **C, E.** Examples of flake detection times (black dots) of a group of 3 fish (C) and a group of 6 fish (E) and the average and standard deviation of the best-fit models (bold colored lines represent averages, shaded areas represent SD). Left: *IND* model representing groups of independent searchers (Red). Right: *ATT* model representing groups of socially attracting agents (Blue). **D, F.** Increase in likelihood by the *ATT* model compared to the *IND* model given by likelihood ratio between the two models (eq. 2); boxplots show the median likelihood ratio and the 1st and 3rd quartiles. Dotted lines represent equality between model likelihoods.

We then compared the feeding rates of foraging fish in simulated groups with attraction and without it, for a wide range of model parameter values (D_f, D_n) (Fig. 5A). Again, the feeding rates were accurately approximated with an exponential fit (as in Eq.

1)($R^2 > 0.98$ for all simulations). As might be expected, the simulated groups consumed flakes faster as D_f increased (Fig. 5B). For relatively low flake detection ranges ($D_f < 7$ BL), flake consumption rates also increased as D_n increased, but for $D_f > 6$ BL, increasing D_n had very little effect on consumption rates (Fig. 5B).

Comparing the *ATT* model to simulated independent foragers, we found a significant increase in consumption rates only for simulations with low D_f and high D_n values (red areas in Fig. 5C). Importantly, most of the groups of real fish were best matched by simulated groups with parameter values that were well within the area of the parameter space were social interactions improve foraging efficiency (low D_f and high D_n), approaching the peak of the expected improvement in foraging performance (Fig. 5C). Moreover, the expected improvement for real groups over independent foragers, was correlated with the value of D_n that best described foraging in these groups (Fig. 5D), suggesting that groups with larger social detection range were also more efficient. Repeating the analysis using the groups' average flake consumption times, and not the rates extracted from the exponential fits, gave very similar results with increased efficiency due to social foraging confined to low D_f values and high D_n values (Fig. S5A).

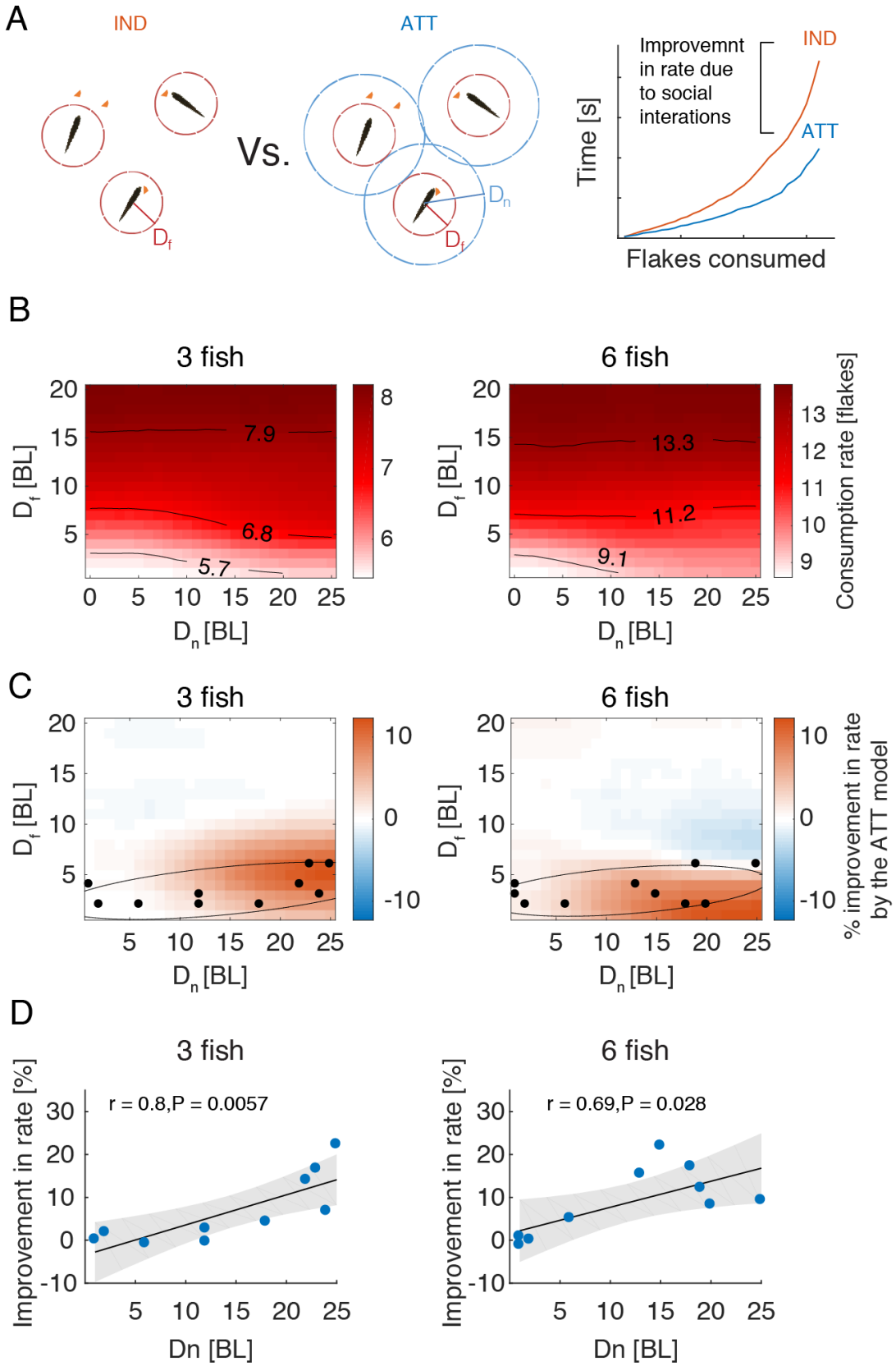

Figure 5: Foraging efficiency of socially attracting fish approach the expected optimal rates. A. *Left*: Sketch of two groups of 3 fish foraging, with their different interaction ranges

D_f, D_n overlaid. For $D_n = 0$ the group is composed of independent foragers (*IND*). *Right*: foraging efficiency was estimated by comparing the slope (*b*) of the exponential function fitted to the rate of flake consumption of attracted (*ATT*) and independent (*IND*) foragers. **B.** Average consumption rates, *b*, for different combinations of D_f and D_n, the first column on the left ($D_n = 0$) represent independent foragers. Contours denote 10, 50, and 90% of the highest observed rate. **C.** Difference in foraging efficiency for groups that utilize social attraction (*ATT*) compared to groups of independent foragers (*IND*) for all model parameters. Dots represent D_f and D_n values of simulated groups that best fitted real foraging groups, and the black ellipse delineate 90% of the groups fitted. **D.** Improvement in foraging rates due to social interactions increases linearly with the range of neighbor detection (D_n) in simulations that best fitted real groups of 3 and 6 fish (shaded area is the 95% confidence interval of the linear regression model in black).

We next explored how prospective social strategies would affect the foraging success of individual members of the group. To address this question, we simulated the same groups but with different individual strategies of the agents within the same group (Fig. 6A illustrates the mixed strategy groups). Specifically, we varied the number of individuals that used a social attraction strategy out of the total number of foragers in the group and compared the foraging success of the social and non-social individuals within the same group (Fig. 6B-C and S6A-C). We found that individuals using social information consumed up to 20% more flakes than their non-interacting companions. This advantage decreased as the number of interacting agents in the group increased (Fig. 6B-C). These effects were most pronounced in models that used the same parameter range that matched real foraging groups – i.e. low D_f values and high D_n ones (Fig. S6A-B). Our results suggest that members of a group should use both their own sensory information about food availability, and information extracted from the behavior of others to increase their foraging success.

Finally, we assessed the equality of food distribution among individuals in real groups and simulated groups using the Theil index of inequality [50]:

$$I_{Theil}(k,n) = \frac{1}{k}\sum_{i=1}^{k}\frac{n_i}{\mu}log\left(\frac{n_i}{\mu}\right) \quad (3)$$

where k is the number of fish in the group, n_i is the number of flakes consumed by the ith fish, and $\mu = \frac{n}{k}$ is the average number of flakes consumed by a fish in the group. We normalized I_{Theil} by its maximal possible value, $log\ k$ (the case where one fish consumes all flakes), and measured equality using $1 - \frac{I_{Theil}}{log\ k}$, which ranges between 0 (a single fish who consumed all flakes) and 1 (full equality). Real groups showed relatively high equality values (Fig. S6D, Median = $0.89\ [0.21], 0.92[0.16]$ for groups of 3 and 6 fish; interquartile range in brackets), indicating that resources were distributed

relatively equally among fish. In simulated groups equality was a function of both the number of socially interacting individuals and the spatial dispersion of the flakes (Fig. S6E-H). For low flake dispersion (i.e. when flakes were more clustered in space), simulated groups composed of just independent foragers showed the highest inequality out of all simulated groups; Equality increased with the number of interacting foragers within the group (Fig. 6D,E). When all individuals in the group used both individual and social information, equality levels were higher than in groups of independent foragers for groups of 3 and 6 fish, for most parameter values that match real foraging groups. In contrast, in environments with high dispersion of flakes these effects disappeared or even reversed with groups of 3 fish showing only a moderate non-significant increase in equality, and groups of 6 fish showing a significant decrease in equality. Thus, only when resources are hard to come by, employing a social attraction strategy increases income equality among group members.

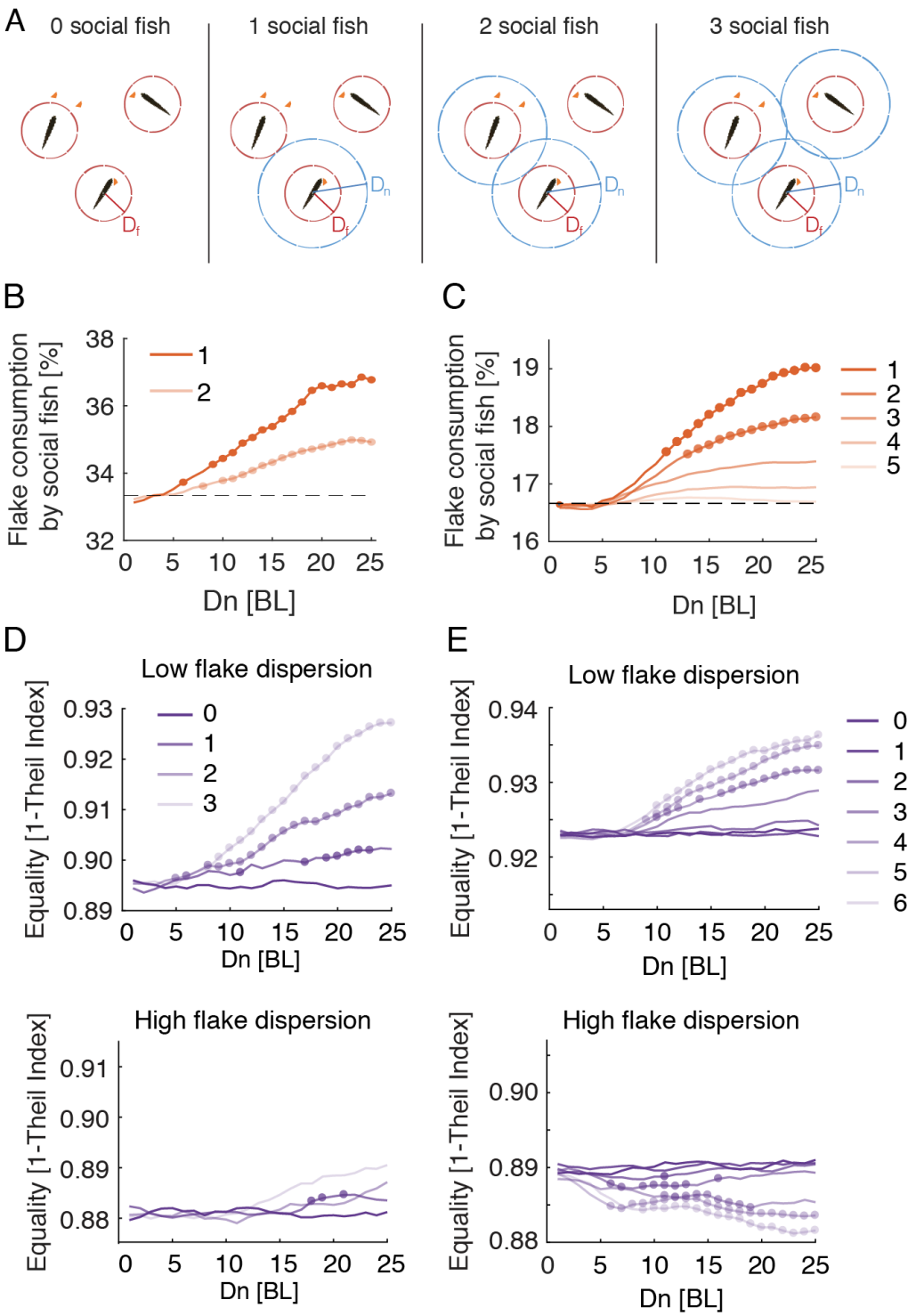

Figure 6: Social interactions promote foraging efficiency and income equality within groups. A. Sketch showing simulated groups of 3 fish with a varying number of foragers who employ a social strategy out of the total members of the groups. **B, C.** Average fraction of flakes consumed by the interacting individuals in the same simulated group. Colors indicate the number of social foragers in the group; dotted line show the expected consumption values in case of full equality; results were averaged over all simulations with $D_f \leq 6$, which was the parameter range where real groups were matched by simulations;

dots represent significant increase in efficiency of foragers over non-foragers within the group (t-test for matched samples, N=10, 10). **D, E.** Equality of food distribution within groups, measured by $1 - \frac{I_{Theil}}{log\ k}$ (Eq. 3). Lighter colors represent a larger fraction of social foragers. Data is shown for both low flake dispersion environments (top), and high dispersion (bottom)(Fig. S6E). Equality values were averaged over $D_f \leq 6$; dots show a significant difference from independent foragers (0 social fish)(Wilcoxon's sign rank test N=5 for each group size and dispersion level).

Discussion

We studied free foraging behavior in groups of zebrafish and found that foraging fish responded to the salient swimming maneuvers of shoal mates that indicated the presence of food, by swimming to these locations [18, 36, 51]. Mathematical models based on social attraction accurately described fish foraging behavior and their success rates. The models also predicted near optimal foraging efficiency for the range of parameters that best match real foraging groups. At the individual level, our simulations show that group members using both private and social information consumed more food than shoal mates that rely only on private information, and that these strategies are robust to different resource densities. Our results show that a simple social foraging heuristic that matches fish behavior in a naturalistic context increases both foraging efficiency and income equality, which can constitute an evolutionary stable strategy [52].

Our modeling focused on vision as the main venue of information flow between fish, since zebrafish rely heavily on their visual system [53, 54]. It is possible, and likely, that other sensory modalities, namely tactile or odor signals, also play a role in information transfer during foraging. Yet, in our analysis the inferred parameters of the best fit models indicated that neighbor detection ranges were ~4 times larger than flake detection ranges (up to 15 Body lengths). It seems less likely that odor or tactile information can be detected from such large distances on such short time scales [55]. In addition, we found that fish showed similar tendency to attract to their neighbors during pseudo detection events, which seems to preclude the possibility that the fish are responding to the physical trace of the flakes. Taken together these findings suggest that fish respond to the prominent visual signal coming from their shoal mates.

We focused on analyzing an attraction-based strategy for the fish, since in our experiments fish were attracted to areas where neighbors detected food. However, previous studies have suggested other search strategies based, for example, on repulsion between individuals [56] or on maximizing information [10]. Although our modeling framework gave an excellent fit to the data, it is possible that foraging fish combine or alternate between strategies in different environmental conditions, based on group composition or their internal state [37, 38, 57]. Models that incorporate additional strategies according to an explicit policy, might prove to be even more accurate in explaining fish behavior.

Empirical observations of groups in nature, and consequent models, suggest that groups contain a fraction of individuals whose search is based on their personal information (``producers”) and a fraction of individuals that rely mostly on social information (``scroungers”) [25, 42, 58]. Our results suggest that when individuals in the group have similar foraging capabilities, and a limited social interaction range [27,

59], using both individual and social information is the most efficient strategy for the individual. We did not find adverse effects of this strategy in terms of increased inequality among members of the group, that may hinder social foraging [18, 51]. Moreover, in environments with low dispersion of resources such that food is harder to come by, a larger fraction of socially interacting individuals within the group meant higher equality of food income among members. Taken together, these results suggest that combining personal and private information may be the preferable strategy by individuals and can represent an evolutionary stable strategy [52].

Finally, we note that our work reflects the power of detailed behavioral analysis of individuals in a group for building mathematical models of social interactions. The data-driven models we built allowed us to explore the efficiency and robustness of the interactions among group members. With increased technical capabilities to monitor social behavior of large groups of individuals, this approach would be applicable to other social foraging species and other foraging tasks. Converging evidence from different species can potentially help revise and refine common theoretical models of social foraging and their underlying assumptions.

Acknowledgments

We thank Udi Karpas, Ori Maoz, Oren Forkosh, Tal Tamir, Adam Haber, Gasper Tkacik, Yadin Dudai, Ofer Feinerman and Iain Couzin for discussions and suggestions. This work was supported by a HFSP grant, European Research Council Grant 311238, and Israel Science Foundation Grant 1629/12, as well as research support from Martin Kushner Schnur and Mr. and Mrs. Lawrence Feis.

Author Contributions: RH and ES designed research, performed research, analyzed data, and wrote the paper.

The authors declare no conflict of interst.

Methods

Experimental setup. Detailed description of the setup is given in [49]. Briefly, adult fish were purchased from a local supplier (Aquazone LTD, Israel) and housed separately in their designated groups for more than a month prior to behavioral experiments. Fish were housed in a standard fish holding system consisting of a recirculating multistage filtration system where temperature, conductivity, PH, and light- dark cycle were monitored.
Imaging of fish foraging behavior was done using an industrial recording system composed of a *Vieworks VC-2MC-M340* camera with an 8 mm lens, a *Karbon-CL* frame grabber, and a recording server. Camera was suspended 150 cm above the experimental tank. During experiments we changed the effective experimental tank size by using different size arenas (Fig. S1A and see below). All water conditions were similar between the holding tanks and the experimental tank.

Fish acclimation and behavioral experiments. To facilitate food searching behavior and to lower fish anxiety, the following acclimation procedure was followed: On day 1, all fish were transferred to the designated experimental tank (D = 95cm; water depth of 5 cm) and were allowed to explore the tank for 5 minutes. On days 2-5, all groups and individual fish were transferred from their home tanks to test tanks of increasing size (Fig. S1A) where 6, 12, or 18 flakes were randomly scattered on the water surface (for groups of sizes 1, 3, and 6 respectively). Fish were first placed in a small starting box (25x25 cm) that was inside a larger arena. The small box was raised after 5 minutes and the fish were allowed to forage and consume the flakes in the larger box for an additional 5 minutes. After the allotted time ended the fish were netted and returned back to their home tanks, keeping their original groups. Over the 4 days of training, we increased the size of the test tank from the small start box itself (day 2) to the largest arena with D = 47.5, 67.2, 95cm on days 3-5 (Fig. S1A). On days 6-7 fish were deprived of food and kept in their home tanks. Foraging was then tested on day 8. During training, no food was administered to the fish outside of the experimental arena. In total, *n = 106* adult fish (3 months old or older) were used at approximately 1:1 male to female ratio. 16 single individuals were tested, 10 groups of 3 fish (30 fish in total), and 10 groups of 6 fish (60 fish in total). Two single individual fish were excluded from analysis as they did not swim when transferred to the experimental tank.

Data extraction. Recorded videos were analyzed off-line to extract the size, position, speed, and orientation of individual fish, and the position of food flakes. Position data was then used to estimate fish trajectories using a designated tracker. All image processing and tracking were done using MatLab© with software written in house; the details of these procedures are described in [49]. Fish identities were further corrected using *IdTracker* [44]. Fish trajectories were smoothed using a Savitzky-Golay filter [60] spanning 17 frames which constituted ~1/3 of a second (all videos were recorded at 50 fps). Fish positions were defined as the coordinates of the center of each fish, $\vec{x}_i(t)$, and fish velocity was calculated as the difference between two consecutive time points: $\vec{v}(t)_i = \vec{x}_i(t) - \vec{x}(t-1)_i$. Direction of motion of the fish was defined as ,

$\vec{d}_i(t) = \frac{\vec{v}_i(t)}{|\vec{v}_i(t)|}$and the trajectory's curvature at time t was given by $c(t) = 1/R(t)$, where R is the radius of the circle that gave the best Euclidean fit to a trajectory segment of length 600 ms, centered on time t.

Flake locations. Flakes' location were tracked with the same methods used for tracking the fish.Flakes disappeared when eaten, and new (sub)flakes sometimes appeared when consumed flakes broke into smaller pieces. Consumption events were defined at times when a fish passed directly over a flake, rendering it invisible to the camera. Our camera resolution did not allow us to confirm whether the fish indeed digested the flake.

Tendency to attract to real flake consumption events. We estimated the probability of fish to cross near locations of consumption events by another fish, $P(crossing)$, by counting all events where at least one fish passed within 2 BL of that location within 1s of a neighbor's flake consumption, and dividing it by the total number of consumption events. Since zebrafish tend to swim in groups, regardless of the presence of food, we compared this number to the probability of one fish to cross near a neighbor's position within 1s when no food was present. We therefore estimated $P_{null}(crossing)$ by drawing k random fish positions (mimicking k flake detection events) 10000 times, from times when no flake was detected for at least 4s (Fig. 2D). The tendency to attract to flake position was then given by: $P(crossing) - \langle P_{null}(crossing) \rangle$.

Tendency to attract to pseudo consumption events. We defined ``pseudo flake consumptions" at times when fish exhibited a similar speed profile to that of a fish during real consumption events, namely gradual increase in speed followed by a sudden sharp decrease back to baseline (Fig. 2B). To detect such events, we convolved the speed profile of individual fish in the group when no flakes were present near the fish with the calculated average speed profile near all real flake consumption events of that group (Fig. 2B) and obtained a correlation measure for each point in time. We then treated the top 2.5 percent of this distribution as pseudo consumption events. The average number of events was 12.6 ± 4 and 21.8 ± 6.6 for groups of 3 and 6 fish, respectively. We compared the probability of neighbors to cross near the locations of such events, $P(pseudo\ crossing)$ to $P_{null}(crossing)$. The tendency of neighboring fish to cross near pseudo consumption events was high, and was correlated with their tendency to cross near real flake consumption events over groups (Fig. S2C, D).

Segmentation of fish trajectories. Segmentation of trajectories into discrete steps was based on the detection of local minima in the speed profile of the fish (Fig. 3A-B). We characterized discrete steps by the total distance traveled between two minima points, *L*, and the change in angle between successive steps, or turning angle, θ. These distributions were estimated for each fish and used to simulate their swimming behavior (Fig. S3A-B).

Simulating fish swimming behavior.

a. Motion. We modeled fish swimming behavior as a random walk, defined by the distribution of step sizes, *L*, and of turning angles between consecutive steps θ (see above). At each time point, we drew for each simulated fish a step size and a turning angle defining the direction of motion and the length of the next step (Fig. 3B, Fig. S3A-B). For all simulated groups, the starting positions of fish matched those of real fish groups. All simulations were conducted within bounded arenas, identical to those used for testing real fish. If a simulation step was expected to end outside of the arena boundaries, that movement was discarded and a new movement was chosen that did not exceed the arena boundaries. To compare simulated foraging time (counted as discrete steps) to real foraging experiments (Fig. 4) we divided the length of each simulated step by the calculated average speed of real foraging fish.

b. Simulated Flakes. In all simulations we used the true positions of flakes as extracted from fish foraging experiments. If a flake drifted during an experimental epoch (due to water turbulence), we only used its final position in the simulations since the speed and distance were negligible compared to the motion of the fish. Since real flakes sometimes disintegrated into smaller bits after a consumption event, we copied that in the simulations. I.e. if flake *i* at position $\vec{x}_i$ has appeared after flake *j* was (partially) consumed, so did the corresponding flakes in the simulation.

c. Sensory range of flake detection. Each simulated fish had a circular range D_f, within which, it could detect a flake, and orient towards it with probability p(go to flake) = e^{-d_f/D_f}, where d_f is the distance to the flake (Fig. 3C). If the fish oriented itself towards the flake, its next step size was drawn from the empirical distribution. If the fish reached the flake (or passed it) during this movement, that flake was considered as consumed. If the simulated fish did not reach the flake, the procedure was repeated. In the *IND* foraging model, *k* such fish were simultaneously simulated, independent of one another.

d. Sensory range of neighbor detection. Because of the tendency of fish in real groups to move towards areas of previous flake consumptions, we allowed fish in our simulated attraction model (*ATT*) to detect and respond to neighbors' previous flake consumption events. Specifically, if a neighbor within the sensory range of neighbor detection, D_n, found a flake in the previous τ time steps, the current fish will orient towards the position of the previous consumption with probability p(go to consumption) = $e^{-\frac{d_n}{D_n}}$, where d_n is the distance to the position where a flake was consumed by a neighbor. In case a movement towards a consumption position was successfully drawn, the fish oriented directly towards that position, and the step size was drawn from the empirical distribution.

e. Hierarchical nature of the social models. In the simulation, if a flake was within the D_f range of a fish, that fish would turn towards it with p(go to flake). If a flake was not detected (i.e. no flake was within D_f), and a neighbor consumed a flake at a distance smaller than D_n, then the fish would move towards that location with the appropriate probability. If neither a flake or a neighbor consumption event were detected, or if motion towards these areas was not successfully drawn, then the next direction of motion of the fish was randomly chosen from the empirical turning angle distribution.

f. Mixed strategy groups. In simulations of groups with mixed individual strategies, fish that used the social attraction followed the procedure described above and the rest used independent foraging (Fig. 6A).

G. model parameters:

	IND	*ATT*
Df – flake range	*1-20 body length, increments of 1*	*1-20 body length increments of 1*
Dn – neighbor range	*0 body length*	*1-25 body length increments of 1*
τ – memory of a neighbor detecting flakes		*5 time steps*
Arena Radii	*32 BL*	*32 BL*
Turning angles	*Estimated from swimming data of each fish*	
Step sizes	*Estimated from swimming data of each fish*	
Flake positions	*According to the starting position and appearance and disappearance dynamics of in experiments.*	
Agents starting positions	*According to the starting positions in experiments*	

Model Fitting. Models were fitted to data by finding the parameter values (D_f for the *IND* model, and D_f, D_n for the *ATT* model) that maximized the log-likelihood of the simulated consumption times given the empirical consumption times of a given group (eq. 2). Specifically, we calculated the probability of the observed consumption time of each flake under the simulated distribution of search times obtained by repeating the simulation procedure 100 times for each parameter combination (see main text). We used kernel density smoothing to estimate a continuous probability from the discrete distribution obtained from simulations.

Mean squared error of the model. We also assessed the models' accuracy by calculating the mean squared error between real flake consumption times and those found in model simulation as:

$$MSE(lnT_{data}, lnT_{sim})_{D_f,D_n} = \langle (lnT_{data} - \langle lnT_{sim}(D_f, D_n)\rangle)^2\rangle$$

where $T_{data}$are real flake consumption times, T_{sim} are simulated time and $\langle \ldots \rangle$ is the average operation. Since flake consumption times grow exponentially during the search (eq. 1) using lnT in this calculation allowed us to achieve a similar magnitude of the error for all k flakes in a given trial (Fig. 1B).

Estimating the expected lower bound of MSE values. To estimate how well simulations of the social model can be expected to fit real data, we calculated the expected MSE values when fitting the ATT model to randomly chosen instantiations of the model itself. We therefore used for each of the real groups 2000 random simulated searches from the total available simulations of the ATT model (for each group there were 100 simulations for every combination of D_f, D_ngiving 62,500 simulation in total). Each of these simulated searches was treated like an instantiation of a real foraging group that was then fitted using the ATT model by searching the D_f, D_n values that will minimize

the MSE (see above). The distributions of these 2000 MSE values for each of the groups were uni-model, typically with a long tail. We then repeatedly sampled N 'groups' from these MSE distributions to mimic N real groups and calculated the median expected MSE. Fig. S4A shows the mean and 95% confidence interval of this expected error distribution.

Measuring flake clustering. To quantify the spatial clustering of flakes, we simulated the random positions of N flake consumptions (corresponding to the number of actual flake consumptions of each of the real groups). We then calculated the average nearest neighbor distance of the simulated flakes D_{nn1}^{rand} and repeated this analysis 100,000 times to obtain a distribution of average nearest neighbor distances expected at random. We then compared the actual average nearest neighbor distance D_{nn1} of flake consumptions to the random distribution and assessed how likely it is to obtain D_{nn1} if flakes were randomly distributed in space. The level of clustering of group k is then defined by: $\widehat{D}(k) = \frac{nn1(k) - \mu_{D_{nn1}^{rand}}(k)}{\sigma_{D_{nn1}^{rand}}(k)}$, where $\mu_{D_{nn1}^{rand}}$ and $\sigma_{D_{nn1}^{rand}}$ are the mean and standard deviation of the distribution of nearest neighbor distances of randomly distributed flakes.

Inequality measure. To quantify the inequality of flake consumptions between members of the same group, we calculated the *Theil* index of inequality [50]. This is an information theory-based measure, assessing the difference in the entropy of a distribution from the maximum entropy expected if consumption rate was equal for all agents. This is given by

$$I_{Theil}(k,n) = \frac{1}{k}\sum_{i=1}^{k}\frac{n_i}{\mu}log\left(\frac{n_i}{\mu}\right)$$

where k is the number of agents, n_i is the number flakes consumed by fish i and μ is the mean number of flakes consumed by a fish in the group. In addition, we normalized I_{Theil} by $log\ k$, the maximum possible value if one fish consumed all flakes. We then quantified equality by, $1 - \frac{I_{Theil}}{log\ k}$, where 1 indicates full equality and 0 is full inequality.

References:

1. Danchin É, Giraldeau L-A, Valone TJ, Wagner RH (2004) Public Information: From Nosy Neighbors to Cultural Evolution. *Science* 305(5683):487–491.
2. Pitcher TJ ed. (1986) *The Behaviour of Teleost Fishes* (Springer US, Boston, MA).
3. Berdahl A, Torney CJ, Ioannou CC, Faria JJ, Couzin ID (2013) Emergent Sensing of Complex Environments by Mobile Animal Groups. *Science* 339(6119):574–576.
4. Miller MB, Bassler BL (2001) Quorum sensing in bacteria. *Annu Rev Microbiol* 55:165–199.
5. Pratt SC, Mallon EB, Sumpter DJ, Franks NR (2002) Quorum sensing, recruitment, and collective decision-making during colony emigration by the ant Leptothorax albipennis. *Behav Ecol Sociobiol* 52(2):117–127.
6. Ward AJW, Herbert-Read JE, Sumpter DJT, Krause J (2011) Fast and accurate decisions through collective vigilance in fish shoals. *Proc Natl Acad Sci* 108(6):2312–2315.
7. Clutton-Brock TH, et al. (1999) Selfish Sentinels in Cooperative Mammals. *Science* 284(5420):1640–1644.
8. McGowan KJ, Woolfenden GE (1989) A sentinel system in the Florida scrub jay. *Anim Behav* 37:1000–1006.
9. Chittka L, Muller H (2009) Learning, specialization, efficiency and task allocation in social insects. *Commun Integr Biol* 2(2):151–154.
10. Karpas ED, Shklarsh A, Schneidman E (2017) Information socialtaxis and efficient collective behavior emerging in groups of information-seeking agents. *Proc Natl Acad Sci* 114(22):5589–5594.
11. Ward AJW, Krause J, Sumpter DJT (2012) Quorum Decision-Making in Foraging Fish Shoals. *PLoS ONE* 7(3):e32411.
12. Shklarsh A, Ariel G, Schneidman E, Ben-Jacob E (2011) Smart Swarms of Bacteria-Inspired Agents with Performance Adaptable Interactions. *PLoS Comput Biol* 7(9):e1002177.
13. Gordon DM (1996) The organization of work in social insect colonies. *Nature* 380(6570):121.
14. Pitcher TJ (1986) Functions of Shoaling Behaviour in Teleosts. *The Behaviour of Teleost Fishes*, ed Pitcher TJ (Springer US, Boston, MA), pp 294–337.
15. Radakov DV (1973) *Schooling in the Ecology of Fish* (John Wiley & Sons Inc).
16. Giraldeau L-A, Caraco T (2000) *Social Foraging Theory* (Princeton University Press).
17. Zahavi A (1971) The Function of Pre-Roost Gatherings and Communal Roosts. *Ibis* 113(1):106–109.
18. Brown CR (1988) Social foraging in cliff swallows: local enhancement, risk sensitivity, competition and the avoidance of predators. *Anim Behav* 36(3):780–792.
19. Pitcher TJ, Magurran AE, Winfield IJ (1982) Fish in larger shoals find food faster. *Behav Ecol Sociobiol* 10(2):149–151.
20. Laland KN, Williams K (1998) Social transmission of maladaptive information in the guppy. *Behav Ecol* 9(5):493–499.
21. Johnstone R. A., Dall S. R. X., Giraldeau Luc–Alain, Valone Thomas J.,

Templeton Jennifer J. (2002) Potential disadvantages of using socially acquired information. *Philos Trans R Soc Lond B Biol Sci* 357(1427):1559–1566.

22. Templeton JJ, Giraldeau L-A (1995) Patch assessment in foraging flocks of European starlings: evidence for the use of public information. *Behav Ecol* 6(1):65–72.
23. Coolen I., Bergen Y. V., Day R. L., Laland K. N. (2003) Species difference in adaptive use of public information in sticklebacks. *Proc R Soc Lond B Biol Sci* 270(1531):2413–2419.
24. Coolen I, Giraldeau L-A, Lavoie M (2001) Head position as an indicator of producer and scrounger tactics in a ground-feeding bird. *Anim Behav* 61(5):895–903.
25. Barnard CJ, Sibly RM (1981) Producers and scroungers: A general model and its application to captive flocks of house sparrows. *Anim Behav* 29(2):543–550.
26. Clark CW, Mangel M (1984) Foraging and Flocking Strategies: Information in an Uncertain Environment. *Am Nat* 123(5):626–641.
27. Bhattacharya K, Vicsek T (2014) Collective foraging in heterogeneous landscapes. *J R Soc Interface* 11(100):20140674.
28. Valone TJ (1989) Group Foraging, Public Information, and Patch Estimation. *Oikos* 56(3):357–363.
29. Tania N, Vanderlei B, Heath JP, Edelstein-Keshet L (2012) Role of social interactions in dynamic patterns of resource patches and forager aggregation. *Proc Natl Acad Sci* 109(28):11228–11233.
30. Torney CJ, Berdahl A, Couzin ID (2011) Signalling and the Evolution of Cooperative Foraging in Dynamic Environments. *PLoS Comput Biol* 7(9):e1002194.
31. Clark CW, Mangel M (1986) The evolutionary advantages of group foraging. *Theor Popul Biol* 30(1):45–75.
32. Harel R, Spiegel O, Getz WM, Nathan R (2017) Social foraging and individual consistency in following behaviour: testing the information centre hypothesis in free-ranging vultures. *Proc R Soc B Biol Sci* 284(1852).
33. Krebs JR (1974) Colonial Nesting and Social Feeding as Strategies for Exploiting Food Resources in the Great Blue Heron (Ardea herodias). *Behaviour* 51(1/2):99–134.
34. Flemming SP, Smith PC, Seymour NR, Bancroft RP (1992) Ospreys use local enhancement and flock foraging to locate prey. *The Auk* 109(3):649–654.
35. Miller N, Garnier S, Hartnett AT, Couzin ID (2013) Both information and social cohesion determine collective decisions in animal groups. *Proc Natl Acad Sci* 110(13):5263–5268.
36. Ryer CH, Olla BL (1995) Influences of food distribution on fish foraging behaviour. *Anim Behav* 49(2):411–418.
37. Farine DR, Aplin LM, Garroway CJ, Mann RP, Sheldon BC (2014) Collective decision making and social interaction rules in mixed-species flocks of songbirds. *Anim Behav* 95:173–182.
38. Michelena P, Sibbald AM, Erhard HW, McLeod JE (2009) Effects of group size and personality on social foraging: the distribution of sheep across patches. *Behav Ecol* 20(1):145–152.
39. Aplin LM, Farine DR, Mann RP, Sheldon BC (2014) Individual-level personality influences social foraging and collective behaviour in wild birds. *Proc R Soc B*

Biol Sci 281(1789):20141016.
40. Martínez-García R, Calabrese JM, Mueller T, Olson KA, López C (2013) Optimizing the Search for Resources by Sharing Information: Mongolian Gazelles as a Case Study. *Phys Rev Lett* 110(24):248106.
41. Hamilton IM, Dill LM (2003) Group Foraging by a Kleptoparasitic Fish: A Strong Inference Test of Social Foraging Models. *Ecology* 84(12):3349–3359.
42. Mottley, Giraldeau (2000) Experimental evidence that group foragers can converge on predicted producer-scrounger equilibria. *Anim Behav* 60(3):341–350.
43. Giraldeau L-A, Beauchamp G (1999) Food exploitation: searching for the optimal joining policy. *Trends Ecol Evol* 14(3):102–106.
44. Pérez-Escudero A, Vicente-Page J, Hinz RC, Arganda S, de Polavieja GG (2014) idTracker: tracking individuals in a group by automatic identification of unmarked animals. *Nat Methods* 11(7):743–748.
45. Ballerini M, et al. (2008) Interaction ruling animal collective behavior depends on topological rather than metric distance: Evidence from a field study. *Proc Natl Acad Sci* 105(4):1232–1237.
46. Greenwald E, Segre E, Feinerman O (2015) Ant trophallactic networks: simultaneous measurement of interaction patterns and food dissemination. *Sci Rep* 5:12496.
47. Nagy M, Akos Z, Biro D, Vicsek T (2010) Hierarchical group dynamics in pigeon flocks. *Nature* 464(7290):890–893.
48. Dell AI, et al. (2014) Automated image-based tracking and its application in ecology. *Trends Ecol Evol* 29(7):417–428.
49. Harpaz R, Tkačik G, Schneidman E (2017) Discrete modes of social information processing predict individual behavior of fish in a group. *Proc Natl Acad Sci* 114(38):10149–10154.
50. Theil H (1967) *Economics and information theory* (North-Holland Pub. Co.).
51. Ranta E, Rita H, Lindstrom K (1993) Competition Versus Cooperation: Success of Individuals Foraging Alone and in Groups. *Am Nat* 142(1):42–58.
52. Smith JM (1982) *Evolution and the Theory of Games* (Cambridge University Press, Cambridge ; New York). 1 edition.
53. Saverino C, Gerlai R (2008) The social zebrafish: Behavioral responses to conspecific, heterospecific, and computer animated fish. *Behav Brain Res* 191(1):77–87.
54. Diana Pita BAM (2015) Vision in two cyprinid fish: implications for collective behavior. *PeerJ* 3:e1113.
55. Moore P, Crimaldi J (2004) Odor landscapes and animal behavior: tracking odor plumes in different physical worlds. *J Mar Syst* 49(1):55–64.
56. Tani NP, Blatt A, Quint DA, Gopinathan A (2014) Optimal cooperative searching using purely repulsive interactions. *J Theor Biol* 361:159–164.
57. Kurvers RHJM, Adamczyk VMAP, van Wieren SE, Prins HHT (2011) The effect of boldness on decision-making in barnacle geese is group-size-dependent. *Proc R Soc B Biol Sci* 278(1714):2018–2024.
58. Harten L, et al. (2018) Persistent producer-scrounger relationships in bats. *Sci Adv* 4(2):e1603293.
59. Bhattacharya K, Vicsek T (2015) To join or not to join: collective foraging strategies. *J Phys Conf Ser* 638:012015.

60. Savitzky Abraham, Golay MJE (1964) Smoothing and Differentiation of Data by Simplified Least Squares Procedures. *Anal Chem* 36(8):1627–1639.